Published in final edited form as:
J Vasc Interv Radiol. 2010 July ; 21(7): 1071–1077. doi:10.1016/j.jvir.2010.01.047.

Vascular endothelial growth factor-A, matrix metalloproteinase-1, and macrophage migration inhibition factor changes in the porcine remnant kidney model: Evaluation by MRI

Sanjay Misra, MD, **Khamal D Misra, BS**, and **James F. Glockner, MD, PhD**
Department of Radiology (S.M., J.F.G., A.A.F.), the Division of Vascular Surgery (S.M.), and Division of Cardiovascular Diseases and Internal Medicine (S.M.), Mayo Clinic, Rochester, Minnesota

Abstract

Purpose—To determine the expression of vascular endothelial growth factor-A (VEGF-A), macrophage migration inhibition factor (MIF), and matrix metalloproteinase-1 (MMP-1) in the porcine remnant kidney model and quantify renal blood flow and volume using phase contrast magnetic resonance imaging with magnetic resonance angiography (PC MRI/MRA).

Material and methods—In 23 pigs, the left renal artery was completely embolized using polyvinyl acrylide (PVA) particles and the right kidney partially embolized (remnant kidney) while six pigs served as controls. The animals were sacrificed early (day 3, 7, and 14, N=3), day 24 (D24, N=5), day 37 (D37, N=3), day 42 (D42, N=9), and day 84 (D84, N=3). MRI/PC MRA of the kidneys was performed prior to sacrifice. The remnant and control kidneys were harvested for Western blotting of VEGF-A, MMP-1, and MIF. Blood was removed for BUN and creatinine prior to embolization and at time of sacrifice.

Results—The kidney function after the embolization was characterized by chronic renal insufficiency. The renal artery blood flow, volume, and weight of the remnant kidney increased significantly over time when compared to controls. At early time points, there was increased expression of MIF and MMP-1 followed by an increase in the expression of VEGF-A by day 37 ($P<0.05$ when compared to control). Masson's trichrome staining of the remnant kidney revealed scarring in the tubulointerstitial space.

Conclusions—In this model, renal blood flow and volume increase as the remnant kidney hypertrophies and scars. There is increased expression of MIF, VEGF-A, and MMP-1 in the remnant kidney.

Introduction

Chronic kidney disease affects more than 20 million people in the United States (1). This population is increasing because of the rise in the prevalence of the etiologies of chronic kidney disease including diabetes, hypertension, and obesity (2–5). As a consequence, the number of patients requiring hemodialysis and renal transplantation has increased and more than doubled

Address reprint requests to: Sanjay Misra, MD Associate Professor Department of Radiology Mayo Clinic 200 First Street SW Rochester, MN 55905 Telephone: 507-255-7208 Fax: 507-255-7872 misra.sanjay@mayo.edu.

from 209,000 in 1991 to 472,000 in 2004 (6). Patients with chronic kidney disease are prone to increased cardiovascular complication rates as well as acute and chronic renal failure requiring renal replacement therapy. Understanding the mechanisms responsible for chronic kidney disease is important so that outcomes may improve in patients.

Histologically, kidneys removed from patients with chronic kidney disease demonstrate changes consistent with angiogenesis and inflammation along with glomerulosclerosis and tubulointerstitial fibrosis which results in decline of kidney function (7). It has been hypothesized that these histologic changes are caused by alteration in angiogenic, matrix regulatory, and inflammatory proteins which include vascular endothelial growth factor-A (VEGF-A), matrix metalloproteinase (MMPs), macrophage migration inhibition factor (MIF), and others (8–16). Each of these proteins has been shown to be increased in experimental animal models and in patients with chronic kidney disease.

In order to understand the mechanisms of chronic kidney disease, animal models have been created in which one kidney is removed along with half of the contralateral kidney, termed a remnant kidney model. There have been many different animals used including rats, mice, rabbits, cats, dogs, baboons, and pigs (17–27). The purpose of the current paper was to determine the expression pattern of vascular endothelial growth factor-A, matrix metalloproteinase, and macrophage migration inhibition factor in a porcine remnant kidney model created by embolizing the renal artery (ablation) with polyvinyl acrylide (PVA) particles. We determined the renal blood flow and volume of the remnant kidney using magnetic resonance imaging with phase contrast magnetic resonance angiography (MRI/PC MRA). Increased blood flow occurs in the arterial vasculature supplying the remnant kidney after the nephrectomy (18,28). Finally, the histologic changes in the remnant kidney were characterized.

Material and methods

Study design

The porcine remnant kidney model was created as described later (27). Twenty three castrated juvenile male pigs (40–50 kg, domestic swine, Larson Products, Sargeant, MN) had chronic renal insufficiency created by renal artery embolization as described later (27). The left renal artery was embolized using polyvinyl acrylide (PVA) particles and the right kidney was partially embolized. The animals were sacrificed at early (day 3, 7, and 14, N=3), day 24 (D24, N=5), day 37 (D37, N=3), day 42 (D42, N=9), and day 84 (D84, N=3). MRI/PC MRA was performed prior to sacrifice (see later). Six pigs (40–50 kg) which were age and sex matched were used as controls.

Institutional Animal Care and Use Committee approval was obtained prior to any procedures being conducted. The animals were housed and handled in accordance with the guidelines of the National Institutes of Health (29). Before every procedure, food was withheld from the pigs for 12 hours. Anesthesia was administered as described later (30).

Creation of chronic renal insufficiency by renal artery embolization

Prior to all procedures, animals were kept NPO (nothing per oral) for 12 h. They were initially anesthetized with a combination of 5 mg/kg tiletamine hydrochloride (50 mg/mL) and zolazepam hydrochloride (50 mg/mL), 2 mg/kg xylazine (Bayer, Shawnee Mission, Kansas), and 0.06 mg/kg glycopyrrolate given intramuscularly. To induce additional anesthesia, an intravenous (IV) fluid line was placed in the ear vein for the delivery of zolazepam hydrochloride (5 mg/kg) as needed. During the procedure, the animals were intubated and placed on a positive-pressure ventilator delivering oxygen (3–5 mL/kg) and isoflurane (1%–

3%). The end-tidal CO_2 volume, oxygen saturation, heart rate, electrocardiogram, and blood pressure were monitored throughout the surgical procedure.

Chronic renal insufficiency was created by subtotal renal infarction by embolizing the renal artery (27,31,32). Six French sheaths were placed in the right femoral artery and the left renal artery was selected by using a 5F tapered angled glide catheter (Boston Scientific, Natick, MA). Through this catheter, 150 to 250-μm polyvinyl acrylide (PVA) particles (PVA Contour, Boston Scientific, Boston, MA) were infused until the left renal artery was completely occluded. Next, either the right upper or lower pole artery was selected and the artery which supplied the lesser amount of kidney was embolized. Each pig was extubated, monitored postoperatively, and treated for 5 days with antibiotics to prevent infection and started on normal pig diet (Lean Gain 95, Land O'Lakes, Inc. St. Paul, MN).

Follow-up measurements

A 10-mL blood sample was collected from the femoral vein for measurements of BUN and creatinine prior to embolization and at time of sacrifice.

Magnetic resonance imaging and cine phase-contrast contrast-enhanced magnetic resonance angiography (MRI/PC MRA)

MRI with cine phase-contrast contrast-enhanced MRA was performed prior to sacrifice as described previously (30,31,33). Briefly, kidney volumes and renal artery blood flow were measured. This was performed in 6 pigs which did not undergo embolization to serve as controls for the volume and renal blood flow. Renal blood flow was determined in the renal artery one centimeter distal to the origin as described previously (30,31,33).

Volume of the kidney

Renal volume for both kidneys was estimated by measuring the anterior to posterior, medial to lateral, and superior to inferior dimensions of the kidneys from the reformatted MRA source images. The following formula for an ellipsoid volume was used: $4/3*\pi*(\alpha*\beta*\gamma)/6$ where π is 3.14, α is the length in the anterior to posterior plane, β is the length in the medial to lateral plane, and the γ is the length from the superior to inferior planes.

Kidney harvesting

To harvest the kidney, a retroperitoneal approach was used to remove the kidney. The kidneys were weighed and then snap frozen in liquid nitrogen and stored at −80°C for Western blotting. Normal control kidneys were removed from pigs which did not undergo embolization.

Western blot analysis

Samples were thawed at room temperature (RT) and the remnant and control kidneys were washed 3 × with 1.0-mL washing buffer (0.45 mM Tris, pH 8.5). The kidneys were then sliced with a surgical knife into thin pieces and put into a denaturing buffer (0.5 mM Tris plus 0.1% SDS). An electronic glass grinder was used to homogenize the kidney tissue. The supernatant from this tissue was separated by centrifugation at 14,000 RPM for 10 min. The protein concentration of the supernatant was measured with a Bio-Rad (Hercules, CA) protein assay kit and 100-μgs of protein from each of the remnant and control kidneys was used for Western blotting. Western blotting for vascular endothelial growth factor-A, matrix metalloproteinase-1, and macrophage migration inhibition factor were performed in the remnant kidney and normal kidneys as described elsewwhere (34). Antibodies and antisera used included: macrophage migration inhibition factor (rabbit anti-human, Abcam, Cambridge, MA), vascular endothelial growth factor-A (Santa Cruz Biotechnology, SC-7269, Mouse anti-human), and matrix metalloproteinase-1 (Abcam).

Histologic analysis of the control and remnant kidney

Masson's trichrome staining of the control and remnant kidney was performed at day 28, 37, 42, and 84.

Statistical analysis

All values are expressed as mean ± SEM. Comparisons among early, D24, D37, D42, and D84 animals were performed using a Kruskal-Wallis test. Pair wise comparisons between groups were also performed using Wilcoxon rank-sum tests. Although a non-significant Kruskal-Wallis *P* value would generally be taken as an indication that pair wise tests do not need to be performed because no group is significantly different, we chose to also report the pair wise *P* values due to the small sample size and the importance of identifying trends. A *P* value of . 05 or less was considered statistically significant. SAS version 9, (SAS Institute Inc., Cary, N.C.) was used for statistical analyses.

Results

Embolization procedures

Twenty three animals underwent total nephrectomy of the left kidney (23) and partial embolization of the right lower pole (18) and right upper pole (5).

Serum blood urea nitrogen (BUN) and creatinine

The average BUN prior to embolization was 7.86 ± 0.69 (mg/dL) and increased to 46.5 ± 2.1 early and was 16.5 ± 2.1 24 days after embolization. By day 37, it was 31 ± 5.3 (mg/dL) and remained elevated at 18 ± 4 by day 42 and remained elevated until day 84. The average creatinine followed a similar pattern to that of the BUN. The creatinine prior to the embolization was 1.06 ± 0.11 (mg/dL) and increased to 6.9 ± 0.28 at early time points and was 1.9 ± 0.28, 24 days after the embolization. This remained 2 times higher than the creatinine prior to embolization and all post embolization values were significantly higher than from the pre-embolization value. By day 37, it was 2.73 ± 0.5 and remained elevated at 2.5 ± 0.3 by day 42 and remained day 84.

Angiographic and magnetic resonance imaging

Figure 1 shows the representative imaging findings of the embolization procedure at day 3, day 14, and day 28. The left kidney underwent total nephrectomy and the right kidney (remnant) underwent partial embolization. Over time, the embolized kidney (nephrectomy) decreased in size while the remnant kidney increased in size.

Renal blood flow and volume

Magnetic resonance imaging was used to evaluate the post embolization changes in the kidneys. The volume of the control kidneys which had not undergone embolization was 21.99 ± 1.5 cm^3. As shown in figure 2, the blood flow of the renal artery supplying the total nephrectomy decreased significantly from 204 ± 11 mL/min to 26.4 ± 6.2 by 24 days after embolization. The blood flow of the renal artery supplying the remnant kidney increased significantly from 154 ± 16 mL/min to 257 ± 30. The volume (Fig. 3) of the total nephrectomy decreased significantly from 90.5 ± 7.2 cm^3 to 25.88 ± 7.24 early and remained at an average of 14.5 to 18.5 by day 84. In contrast, the remnant kidney increased from 21.99 ± 1.5 cm^3 to 42.22 ± 2.57 early and continued to increase to 62.49 by day 28–84. By Spearman's rank coefficient, there was statistically significant correlation (P=0.001) between the volume by MRI and the weight of the total nephrectomy with no other correlations being significant.

Kidney weights

By day 24, the mean weight of the remnant kidney was 133 ± 8 g and by day 31 was 143 ± 4 g. By day 37, it had increased to 155 ± 14 and by day 42 was 128 ± 8 and by day 84 was 177 ± 3 g. Over the same time points, the average weight of the embolized kidney decreased.

Protein expression of macrophage migration inhibition factor, matrix metalloproteinase, and vascular endothelial growth factor-A in the remnant and control kidneys at different time points

Protein expression of macrophage migration inhibition factor, matrix metalloproteinase, and vascular endothelial growth factor-A was determined by Western blot on both the remnant and control kidneys to determine the temporal relationship of macrophage migration inhibition factor, matrix metalloproteinase, and vascular endothelial growth factor-A at different time points. Scanning densitometry values from the immunoblots from protein samples of the remnant and control kidneys was determined (Figs. 4–6). The mean macrophage migration inhibition factor expression (Fig. 4) at early time points at less than one week was 2.43 ± 0.25 ($P<0.05$, remnant compared to controls) which decreased by day 24 to 1.17 ± 0.11 and stayed at day 37 (0.92 ± 0.01, $P<0.05$ remnant compared to controls) and 42 (1.14 ± 0.03, $P<0.05$ remnant compared to controls) which increased to 1.97 ± 0.93 by day 84. The mean matrix metalloproteinase −1 expression (Fig. 5) at early time points was 1.44 ± 0.06 ($P<0.05$, remnant compared to controls) which decreased by day 24 to 0.87 ± 0.06 and stayed at day 37 (0.86 ± 0.05, $P<0.05$ remnant compared to controls). By day 42, it was (0.86 ± 0.05, $P<0.05$ remnant compared to controls) and by day 84 increased to 1.09 ± 0.15. At early time points, the mean vascular endothelial growth factor-A expression (Fig. 6) was 1.35 ± 0.22 which by day 24 decreased to 0.62 ± 0.21. By day 37, the mean vascular endothelial growth factor-A increased to 1.98 ± 0.05 ($P<0.05$ when compared to early), by day 42 (1.09 ± 0.24), and day 84 (0.8 ± 0.02, $P<0.05$ when compared to early). Overall, these results indicate an early rise in MIF and MMP-1 followed by VEGF-A.

Masson's trichrome staining in the remnant kidney

Mason's trichrome staining was performed on representative sections removed from the remnant kidney of animals euthanized on day 28 after the embolization procedure and control kidney to determine the scarring in the kidney. The control kidney (left) and remnant kidney (right) columns are shown in figure 7. The normal kidney remains unaltered while there is accumulation of fibrotic tissue in the tubulo-interstitial compartment which is present on day 28 and worsens at later time points (right, 20×). These changes are consistent with the clinical scenario.

Discussion

In the present paper, a porcine remnant kidney model of chronic renal insufficiency was characterized. We determined the changes in the protein expression of matrix metalloproteinase, macrophage migration inhibition factor, and vascular endothelial growth factor-A over time along with changes in renal blood flow and volume using PC MRI with MRA. We observed that the remnant kidney hypertrophies by increasing its volume and renal artery blood flow. Using Masson's trichrome staining, the remnant kidney develops fibrosis and scarring which worsens over time. Finally, there was increased expression of several important proteins implicated in hypertrophy and scarring including matrix metalloproteinase, macrophage migration inhibition factor, and vascular endothelial growth factor-A.

By histologic analysis of the kidney, patients with chronic kidney disease have changes in angiogenesis, inflammation, and scarring. In the late stages of kidney disease, glomerulosclerosis and interstitial fibrosis occur (7). There are two key processes which

contribute to the pathophysiology of kidney disease including changes in angiogenesis and inflammation. In order to understand the mechanisms, remnant kidney models have been used. Hypertrophy with scarring of the remnant kidney is known to occur in several different remnant kidney animal models including cats, dogs, baboons, and pigs (23–27). The histologic examination of the remnant kidney supports the changes observed in the remnant kidney weight. By immunostaining using Masons trichrome, there was increased scarring in the specimens removed from the remnant kidney after day 28 as the kidney settled into a chronic renal insufficiency. Similar histologic results have been observed in kidneys removed from rats that had undergone bilateral renal artery embolization (35).

Proteins involved in inflammation, angiogenesis, and extracellular matrix deposition have been implicated in chronic kidney disease. There have been several proteins implicated including matrix metalloproteinases, macrophage migration inhibition factor, and vascular endothelial growth factor-A; all of which have been involved in angiogenesis and inflammation. Several matrix metalloproteinase have been shown to have increased expression in kidneys including matrix metalloproteinase −1, −2, −3, −8, −9, and −13 (36). It is hypothesized that these proteins lead to extracellular matrix deposition causing scarring which occurs in the remnant kidney model. Recently matrix metalloproteinase-1 was localized to the glomeruli in areas of scarring and shown to be increased in the rat remnant model (14). In the present paper, we determined the expression of MMP-1 in the porcine remnant kidney over time and found that it was significantly increased when compared to the normal kidney at early time points.

A potent stimulator of angiogenesis is vascular endothelial growth factor-A which is also involved in cell proliferation and migration (37). Increased expression of vascular endothelial growth factor-A has been shown to occur in diabetic nephropathy, glomerulosclerosis, and other kidney diseases (37). Increased expression of vascular endothelial growth factor-A has been observed in the remnant kidney and felt to contribute to scarring seen in this model. Furthermore, the use of angiostatin which is a inhibitor of vascular endothelial growth factor-A has shown to decrease extracellular matrix deposition in the rat remnant kidney model (16). In the present study, we observed increased expression of vascular endothelial growth factor-A in the remnant kidney when compared to the control kidney at day 37.

Macrophage migration inhibition factor is a proinflammatory cytokine which is involved in atherosclerosis and chronic kidney disease (8,9). Until recently, there have not been many studies describing the role of MIF in kidney disease. A recent study showed that it was increased in the serum of patients with chronic kidney disease (9). In addition, it has been shown to be involved in kidney disease mediated by immunologic injury (8). In the present study, we observed increased expression of MIF in the remnant kidney when compared to normal kidneys.

The renal blood flow and volume in the remnant kidney after embolization was quantified using MRI. By day 24, when the remnant kidney is compared to controls, the renal artery blood flow in the remnant kidney increased 66% and the renal volume increased 250%. Both of these increases persisted at later time points. These results are in agreement with experiments performed in rats after unilateral nephrectomy in which renal blood flow in the remaining kidney increased more than two fold by 28 days after the nephrectomy (18). By Spearman's correlation rank, there was significant correlation between the volume by MRI and the weight of the total nephrectomy.

There are several limitations of the present study including that glomerular filtration rate and urinary proteins were not evaluated in the animals after nephrectomy. In addition, serial changes in the kidneys following embolization by MRI were not performed. We did not

measure protein expression in the embolized kidney as this provides a negligible amount of kidney function as it has been devascularized.

In conclusion, a porcine remnant kidney model was characterized which had increased expression of matrix metalloproteinase-1, macrophage migration inhibition factor, and vascular endothelial growth factor-A in the remnant kidney when compared to control kidneys. Furthermore, the remnant kidney responds by increasing its blood flow, volume, and weight as hypertrophies and scars over time. The availability of this remnant model will allow future studies to be performed investigating the mechanism of chronic kidney disease using anti-matrix metalloproteinase-1, macrophage migration inhibition factor, and vascular endothelial growth factor-A therapies.

References

(1). Coresh J, Selvin E, Stevens LA, et al. Prevalence of chronic kidney disease in the United States. JAMA Nov 7;2007 298:2038–2047. [PubMed: 17986697]

(2). Gregg EW, Cheng YJ, Cadwell BL, et al. Secular trends in cardiovascular disease risk factors according to body mass index in US adults. JAMA 2005;293:1868–1874. [PubMed: 15840861]

(3). Mokdad AH, Ford ES, Bowman BA, et al. Prevalence of obesity, diabetes, and obesity-related health risk factors, 2001. JAMA 2003;289:76–79. [PubMed: 12503980]

(4). Fields LE, Burt VL, Cutler JA, Hughes J, Roccella EJ, Sorlie P. The burden of adult hypertension in the United States 1999 to 2000: a rising tide. Hypertension 2004;44:398–404. [PubMed: 15326093]

(5). Hajjar I, Kotchen TA. Trends in prevalence, awareness, treatment, and control of hypertension in the United States, 1988–2000. JAMA 2003;290:199–206. [PubMed: 12851274]

(6). US Renal Data Systems. USRDS 2006 Annual Data Report: Atlas of End-Stage Renal Disease in the United States. National Institutes of Health, National Institute of Diabetes and Digestive and Kidney Diseases; Bethesda, MD: 2007.

(7). Fogo AB. Mechanisms of progression of chronic kidney disease. Pediatr Nephrol Dec;2007 22:2011–2022. [PubMed: 17647026]

(8). Lan HY, Bacher M, Yang N, Mu W, et al. The pathogenic role of macrophage migration inhibitory factor in immunologically induced kidney disease in the rat. J Exp Med 1997;185:1455–1465. [PubMed: 9126926]

(9). Bruchfeld A, Carrero JJ, Qureshi AR, et al. Elevated serum macrophage migration inhibitory factor (MIF) concentrations in chronic kidney disease (CKD) are associated with markers of oxidative stress and endothelial activation. Mol Med 2009;15:70–75. [PubMed: 19081768]

(10). Ronco P, Lelongt B, Piedagnel R, Chatziantoniou C. Matrix metalloproteinases in kidney disease progression and repair: a case of flipping the coin. Semin Nephrol 2007;27:352–362. [PubMed: 17533011]

(11). Norman JT, Gatti L, Wilson PD, Lewis M. Matrix metalloproteinases and tissue inhibitor of matrix metalloproteinases expression by tubular epithelia and interstitial fibroblasts in the normal kidney and in fibrosis. Exp Nephrol 1995;3:88–89. [PubMed: 7773643]

(12). Norman JT, Lewis MP. Matrix metalloproteinases (MMPs) in renal fibrosis. Kidney Int Suppl 1996;54:S61–S63. [PubMed: 8731197]

(13). Johnson TS, Haylor JL, Thomas GL, Fisher M, El Nahas AM. Matrix metalloproteinases and their inhibitions in experimental renal scarring. Exp Nephrol 2002;10:182–195. [PubMed: 12053120]

(14). Ahmed AK, Haylor JL, El Nahas AM, Johnson TS. Localization of matrix metalloproteinases and their inhibitors in experimental progressive kidney scarring. Kidney Int 2007;71:755–763. [PubMed: 17290295]

(15). Schrijvers BF, Flyvbjerg A, De Vriese AS. The role of vascular endothelial growth factor (VEGF) in renal pathophysiology. Kidney Int 2004;65:2003–2017. [PubMed: 15149314]

(16). Mu W, Long DA, Ouyang X, et al. Angiostatin overexpression is associated with an improvement in chronic kidney injury by an anti-inflammatory mechanism. Am J Physiol Renal Physiol 2009;296:F145–F152. [PubMed: 18971211]

(17). Heifets M, Morrissey JJ, Purkerson ML, Morrison AR, Klahr S. Effect of dietary lipids on renal function in rats with subtotal nephrectomy. Kidney Int 1987;32:335–341. [PubMed: 3669493]

(18). Sigmon DH, Gonzalez-Feldman E, Cavasin MA, Potter DL, Beierwaltes WH. Role of nitric oxide in the renal hemodynamic response to unilateral nephrectomy. J Am Soc Nephrol 2004;15:1413–1420. [PubMed: 15153552]

(19). Kren S, Hostetter TH. The course of the remnant kidney model in mice. Kidney Int 1999;56:333–337. [PubMed: 10411710]

(20). Fine LG, Schlondorff D, Trizna W, Gilbert RM, Bricker NS. Functional profile of the isolated uremic nephron. Impaired water permeability and adenylate cyclase responsiveness of the cortical collecting tubule to vasopressin. The Journal of Clinical Investigation 1978;61:1519–1527. [PubMed: 207738]

(21). Fine LG, Trizna W, Bourgoignie JJ, Bricker NS. Functional profile of the isolated uremic nephron. Role of compensatory hypertrophy in the control of fluid reabsorption by the proximal straight tubule. The Journal of clinical investigation 1978;61:1508–1518. [PubMed: 659612]

(22). Fine LG, Yanagawa N, Schultze RG, Tuck M, Trizna W. Functional profile of the isolated uremic nephron: potassium adaptation in the rabbit cortical collecting tubule. The Journal of clinical investigation 1979;64:1033–1043. [PubMed: 225350]

(23). Adams LG, Polzin DJ, Osborne CA, O'Brien TD, Hostetter TH. Influence of dietary protein/calorie intake on renal morphology and function in cats with 5/6 nephrectomy. Lab Invest 1994;70:347–357. [PubMed: 8145529]

(24). Bourgoignie JJ, Gavellas G, Martinez E, Pardo V. Glomerular function and morphology after renal mass reduction in dogs. J Lab Clin Med 1987;109:380–388. [PubMed: 3819576]

(25). Brown SA, Navar LG. Single-nephron responses to systemic administration of amino acids in dogs. Am J Physiol 1990;259:F739–F746. [PubMed: 2240229]

(26). Bourgoignie JJ, Gavellas G, Sabnis SG, Antonovych TT. Effect of protein diets on the renal function of baboons (Papio hamadryas) with remnant kidneys: a 5-year follow-up. Am J Kidney Dis 1994;23:199–204. [PubMed: 8311075]

(27). Misra S, Gordon JD, Fu AA, et al. The Porcine Remnant Kidney Model of Chronic Renal Insufficiency. J Surg Res 2006;135:370–379. [PubMed: 16815448]

(28). Wilasrusmee C, Botash R, Da Silva M, et al. Initial angiogenic response in reduced renal mass after transplantation. J Surg Res 2003;115:63–68. [PubMed: 14572774]

(29). Committee on care and use of laboratory animals of the institute of laboratory animal resources. Washington, DC: Government print office; 1996.

(30). Misra S, Doherty MG, Woodrum D, et al. Adventitial remodeling with increased matrix metalloproteinase-2 activity in a porcine arteriovenous polytetrafluoroethylene grafts. Kidney Int 2005;68:2890–2900. [PubMed: 16316367]

(31). Misra S, Fu AA, Puggioni A, Karimi KM, et al. Increased shear stress with up regulation of VEGF-A and its receptors and MMP-2, MMP-9, and TIMP-1 in venous stenosis of hemodialysis grafts. Am J Physiol Heart Circ Physiol 2008;294:H2219–H2230. [PubMed: 18326810]

(32). Misra S, Fu A, Pugionni A, et al. Increased expression of Hypoxia inducible factor-1D in a porcine model of chronic renal insufficiency with arteriovenous polytetrafluoroethylene grafts. J Vasc Interv Radiol 2008;19:260–265. [PubMed: 18341959]

(33). Misra S, Woodrum D, Homburger J, et al. Assessment of Wall Shear Stress Changes in Arteries and Veins of Arteriovenous Polytetrafluoroethylene Grafts Using Magnetic Resonance Imaging. Cardiovasc Intervent Radiol 2006;29:624–629. [PubMed: 16729233]

(34). Misra S, Lee N, Fu A, Raghavakaimal S, et al. Increased expression of a disintegrin and metalloproteinase thrombospondin-1 (ADAMTS-1) in thrombosed hemodialysis grafts. J Vasc Interv Radiol 2009;19:111–119. [PubMed: 18192475]

(35). Miller PL, Rennke HG, Meyer TW. Hypertension and progressive glomerular injury caused by focal glomerular ischemia. Am J Physiol 1990;259:F239–F245. [PubMed: 2386205]

(36). Lenz O, Elliot SJ, Stetler-Stevenson WG. Matrix metalloproteinases in renal development and disease. J Am Soc Nephrol 2000;11:574–581. [PubMed: 10703682]

(37). Schrijvers BF, Flyvbjerg A, De Vriese AS. The role of vascular endothelial growth factor (VEGF) in renal pathophysiology. Kidney Int 2004;65:2003–2017. [PubMed: 15149314]

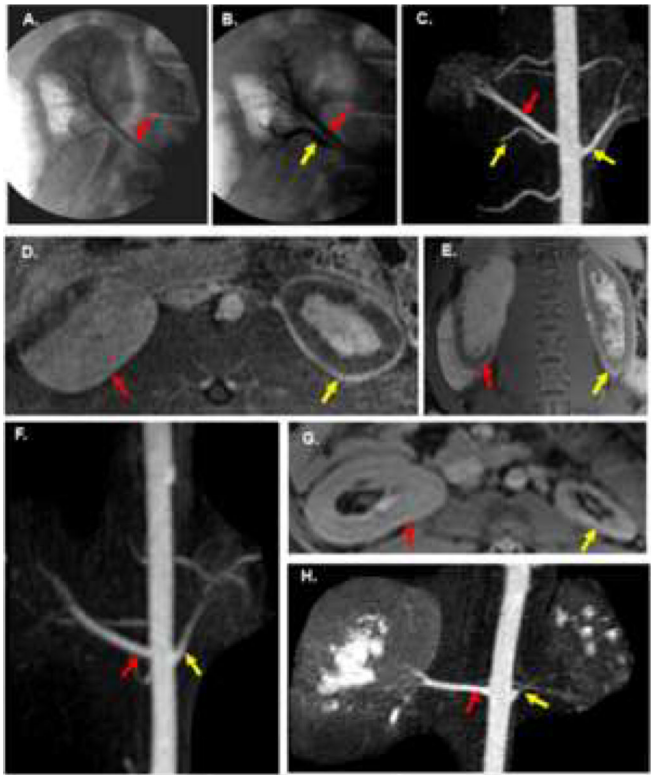

Fig. 1.

Angiographic and MRI findings of renal artery embolization. **A–E** are from the same animal. **A**. Pre embolization angiogram of right kidney shows right upper pole artery (red arrow). **B**. Post embolization angiogram of lower pole (yellow arrow) artery with normal upper pole artery (red arrow). **C–E**. MRI of the kidneys 3 days after embolization. **C**. Subvolume maximum intensity projection image from contrast-enhanced 3D MRA with embolized arteries (yellow arrow) and normal upper pole artery (red arrow) of the remnant kidney. **D**. Axial contrast-enhanced fat-saturated 3D spoiled gradient echo image showing largely intact upper pole of the right kidney (red arrow). Notice the rim of devascularization in the anterior lateral aspect of the remnant kidney. The total nephrectomy (yellow arrow) demonstrates extensive devascularization with only a thin rim of peripheral enhancement and some central enhancement. **E**. Coronal contrast-enhanced fat-saturated 2D SPGR image showing similar findings. Red arrow is remnant (right) kidney and yellow arrow is the total nephrectomy (left). **F**. Coronal subvolume MIP image from CE 3D MRA on a day 14 animal with an enlarged renal artery (red arrow) supplying the remnant kidney and a smaller renal artery (yellow arrow) supplying the total nephrectomy. **G–H** are day 28 images from the same animal. **G**. Axial post-contrast 2D SPGR image shows hypertrophy of the remnant kidney (red arrow) and extensive atrophy of the total nephrectomy (yellow arrow). **H**. MIP image from a 3D CE MRA shows continued enlargement of the renal artery (red arrow) supplying the remnant kidney while the renal artery (yellow arrow) supplying the total nephrectomy has narrowed considerably.

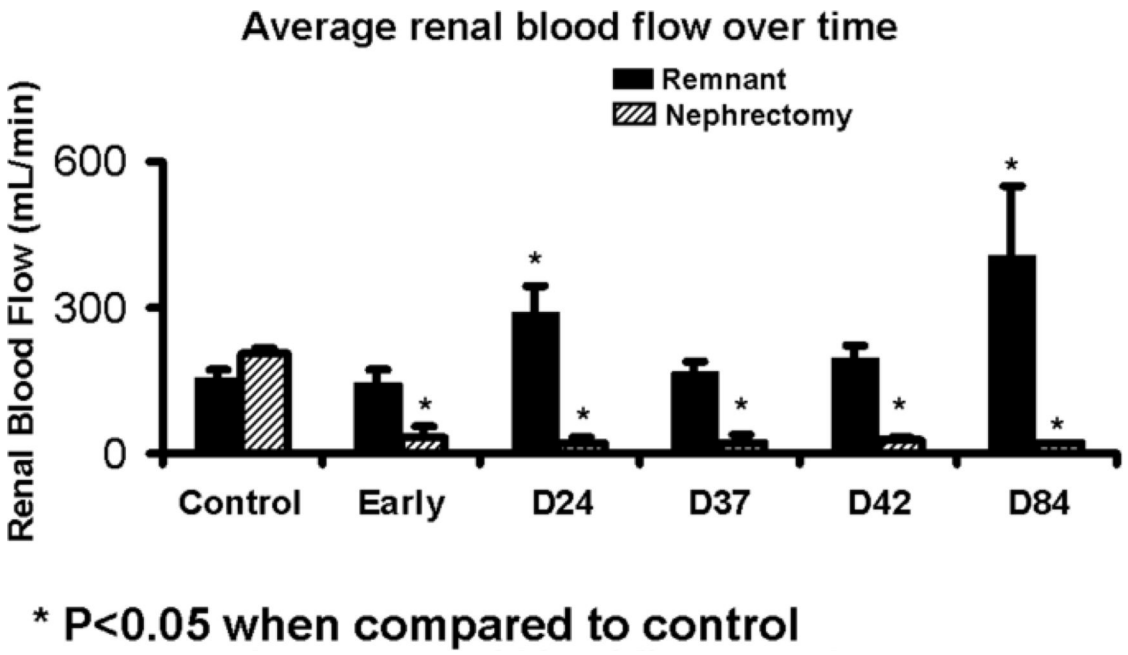

Fig. 2.
Average blood flow of the remnant versus nephrectomy kidneys at different time points.

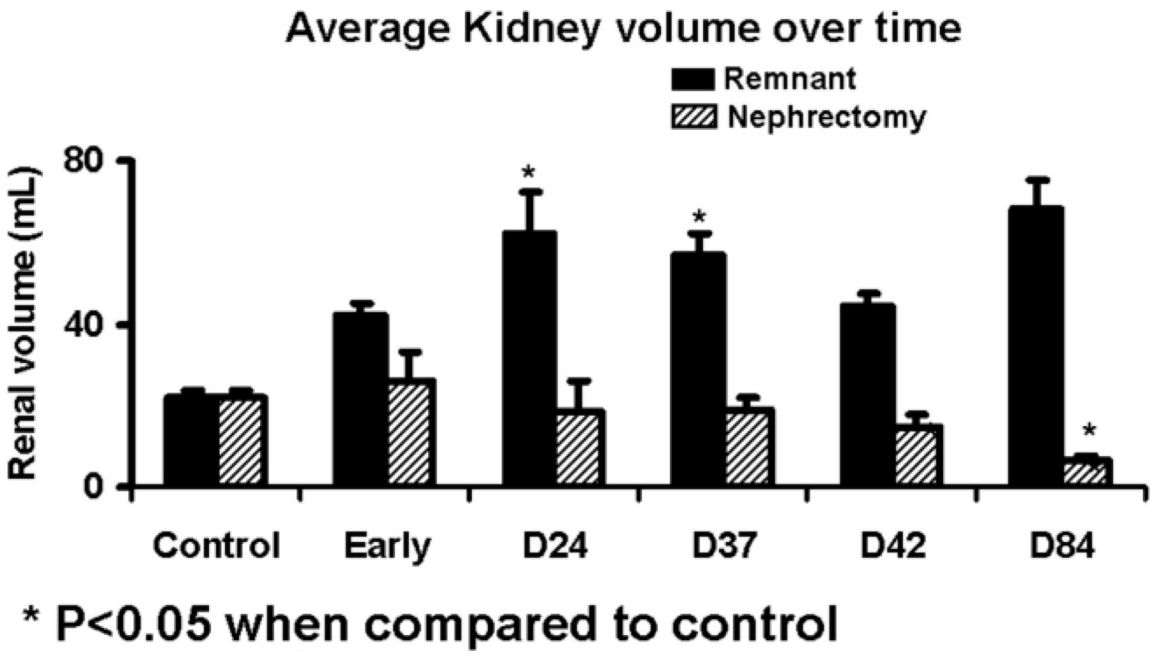

Fig. 3.
Average volume of the remnant versus nephrectomy kidneys at different time points.

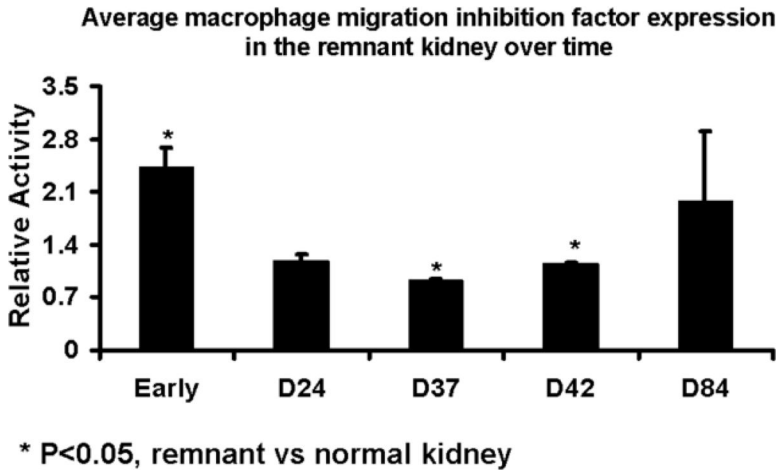

Fig. 4.
Average MIF expression in the remnant versus nephrectomy kidney at different time points

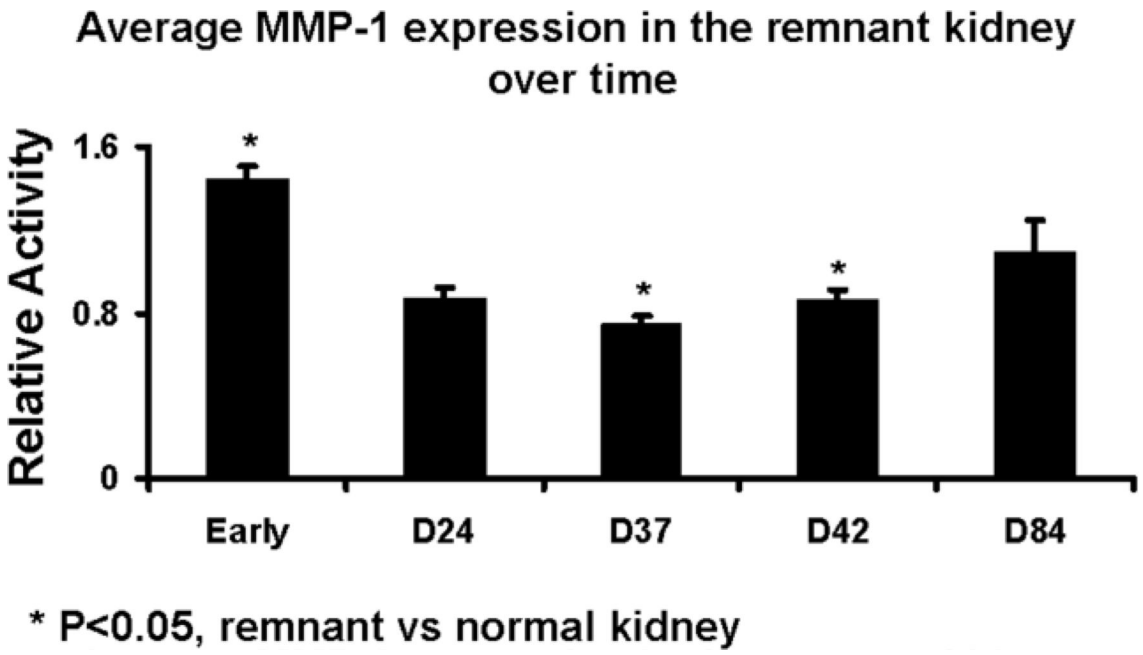

Fig. 5.
Average MMP-1 expression in the remnant versus nephrectomy kidney at different time points

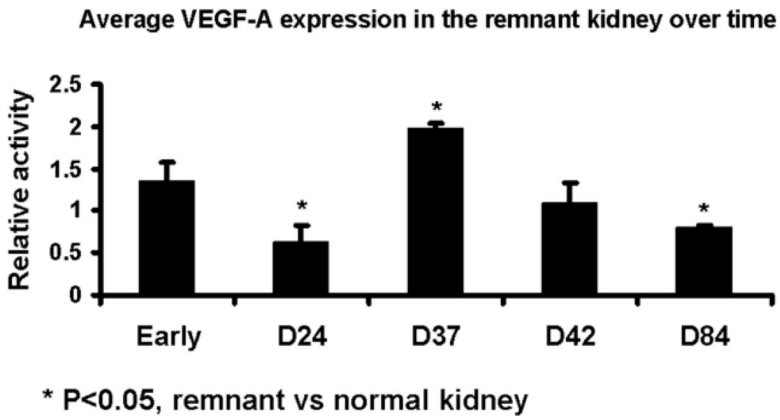

Fig. 6.
Average VEGF-A expression in the remnant versus nephrectomy kidney at different time points.

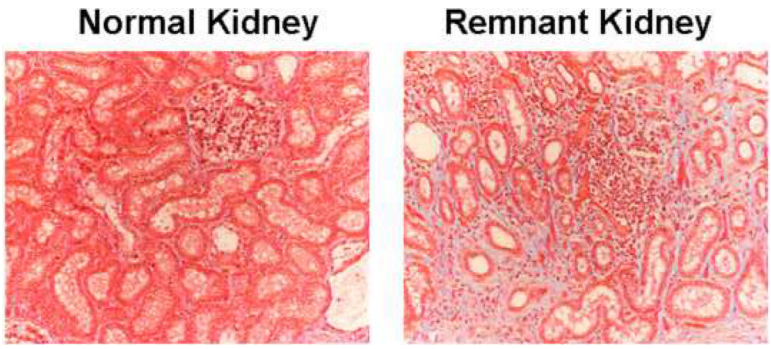

Fig. 7.
Masson's trichrome staining of the control and remnant kidney at day 28